

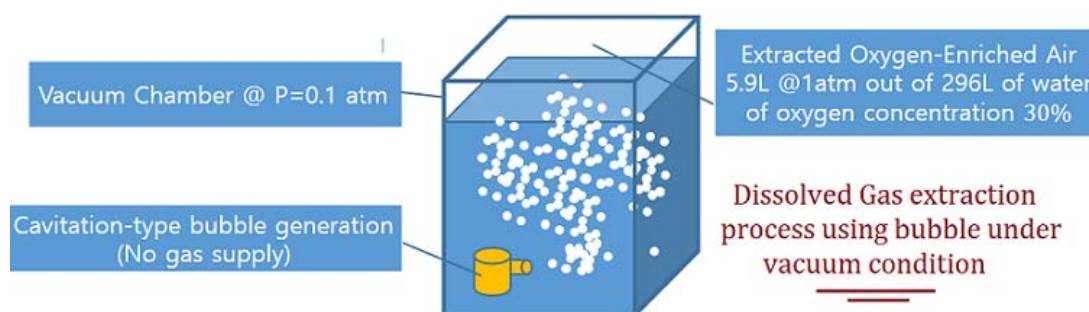
## Extraction of Oxygen-Enriched-Air from Water through Vapor Bubble Diffusion

Jeong-A Hong, Jong-Soo Lee, Yong-Du Jun\*

Department of Mechanical Engineering, Kongju National University, 1223-24 Cheonandae-ro, Seobuk-gu, Cheonan-si, Chungnam-do, 31080, Korea

Received on: 15-Jan-2021, Accepted and Published on: 21-Aug-2021

### ABSTRACT



Present study deals with the method of extracting dissolved gas from water and the characterization of the extracted gas in terms of its oxygen concentration and the possible extractable gas amount. This topic has at least two important aspects; one is on the usability of the extracted dissolved gas from water which is believed to have higher oxygen concentration than the atmosphere, and the other is on the achievable level of deaeration by using the present deaeration method. In the present study, a degassing process based on micro-vapor-bubble diffusion is proposed and theoretically reviewed based on the physical laws such as Henry's law on solubility, Fick's law of diffusion, and the vapor pressure of water as a condition for vapor bubble generation. An experimental apparatus is set up for the present study which is composed of a sealed water tank (0.65m×0.65m×1.0m, stainless steel) with pressure control, a micro-vapor-bubble generator, and the measurement system with sensors for oxygen (for gas mixture) and dissolved oxygen (for water) contents as well as for pressures and temperatures. The limiting extractable amount of dissolved gas from water and the oxygen concentration of the extracted gas mixture is successfully measured for demonstration through the present experimental work. Through the present study, 5.9 liters of extracted gas with oxygen concentration of 30% is captured out of 296 liters of water at room conditions of 17°C and 1 atm.

*Keywords: Dissolved oxygen, Vapor bubble, Gas stripping, Solubility, Degassing*

### INTRODUCTION

Dissolved gas in liquids and its treatment has long been an interesting issue from many and diversified applications such as "artificial gills",<sup>1</sup> deaeration processes in food and beverage industry, and in energy industry.<sup>2-4</sup> The efforts to develop artificial gills<sup>5</sup> include studies to develop underwater breathing systems<sup>6</sup> that can directly extract and separate dissolved oxygen (DO) from water, most approaches of which relies on polymeric membrane

technologies<sup>7</sup> or hollow fibers to obtain DO from pressurized water as noted by Lee et al.<sup>1</sup> One of the key drawbacks of this pressure driven membrane technology is that the process requires significant amount of external energy mainly for pressurization. Deaeration refers to the removal of dissolved gases, such as oxygen, from liquids.<sup>8</sup> Pressure deaerators, known to be the most efficient, and are used in all the power plants, relies its operation on the diffusion of gas between the oxygen-free steam and the sprayed droplets, in which steam not only contributes to the diffusion of gas between the two phases (liquid phase droplets to gas-phase steam) but also heats the fine water droplets near to saturation temperature.<sup>4</sup> Figure 1 illustrates a typical spray deaerator which is composed of highly pressurized feed water inlet, a deaerator vessel with necessary arrangements, steam supply, feed pump and vacuum pump (not shown in the figure), which makes the system a bulky and highly energy consuming one.

\*Corresponding Author: Dr. Yong-Du Jun, Professor, Kongju National University, Cheonan-si, 31080, Korea  
Email: yjun@kongju.ac.kr

Cite as: *J. Integr. Sci. Technol.*, 2021, 9(1), 22-29.

© Authors CC4 By NC-ND Published by: ScienceIN  
IJST ISSN: 2321-4635 <http://pubs.iscience.in/jist>

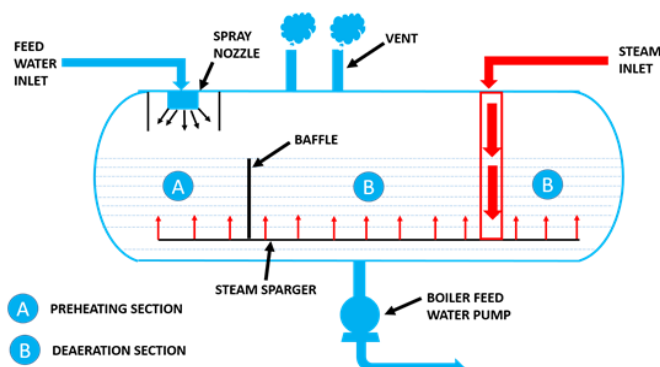


Figure 1. A typical spray deaerator layout. Reproduced from ref [4].

## RELATED PHYSICAL PHENOMENA

### Depressurization and Solubility

Suppose that we have fresh water in a closed tank under an equilibrium condition with a standard air of 20.9% oxygen concentration at 25°C and 1atm, and we lower the tank pressure down by venting out the air in the ullage down to 0.1 atm. According to Henry’s law of solubility which states that the solubility is proportional to the partial pressure of species as

$$G_{aq} = kP_g \tag{1}$$

where  $G_{aq}$  is the solubility (mol/L·atm),  $k$  is Henry’s constant, and  $P_g$  is the partial pressure of a gas (atm), the solubility would decrease to 1/10 of its initial value.

Assuming the idealized atmospheric air is composed of oxygen and nitrogen with volume fractions of 20.9% and 79.1%, respectively, and the partial pressure of water vapor contributes 3.13% of the mixture air, the equilibrium gas concentrations of oxygen and nitrogen in water can be estimated as shown in Figure 2. Table 1 illustrates the selected values of Henry’s constants of oxygen, nitrogen and carbon-dioxide in water under 1 atm at 25°C.

Table 1. Henry’s constants for various gases in water at 25°C.

Henry’s constants in water	Unit	Value
$k_{O_2}$	mol/(L·atm)	$1.28 \times 10^{-3}$
$k_{N_2}$		$6.48 \times 10^{-4}$
$k_{CO_2}$		$3.38 \times 10^{-2}$

$$G_{O_2} \left( \frac{mol}{L} \right) = k_{O_2} P_{O_2} \tag{2}$$

$$G_{N_2} \left( \frac{mol}{L} \right) = k_{N_2} P_{N_2} \tag{3}$$

or

$$G_{O_2} \left( \frac{mg}{L} \right) = k_{O_2} P_{O_2} M_{O_2} \tag{4}$$

$$G_{N_2} \left( \frac{mg}{L} \right) = k_{N_2} P_{N_2} M_{N_2} \tag{5}$$

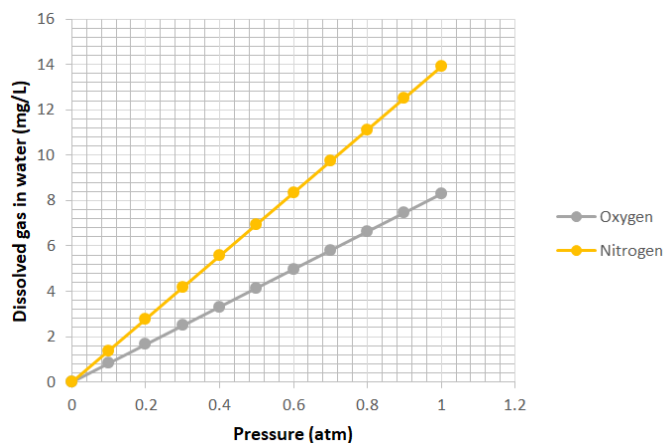


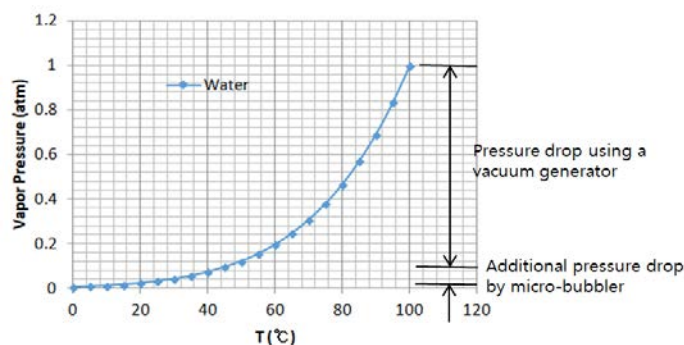
Figure 2. Expected dissolved gas contents (mg/L) of oxygen and nitrogen in water for different atmospheric pressures at 25°C according to Henry’s law under an equilibrium state.

Figure 2 shows the dependency of solubility of oxygen and nitrogen in water on the pressure level indicating that if we lower down the pressure then the solubility limit diminishes linearly with the partial pressure of individual species.<sup>9,10</sup> Now considering water body that is initially saturated with oxygen and nitrogen at 25°C and 1atm and the pressure is lowered down to, for example, 0.1 atm, it is possible that gases may come out of water because of the lowered solubility. The conceivable maximum amount of gases extractable from water can be estimated using Eq.s (2) to (5), that is,  $2.34 \times 10^{-4}$  mol/L of oxygen and  $4.46 \times 10^{-4}$  mol/L of nitrogen, respectively, assuming the equilibrium arrived. Or if we have 1 ton of water at 25°C, the conceivable total amount of extracted gas would be 17.2 L composed of 5.9 L of oxygen and 11.3L of nitrogen, resulting in expected oxygen concentration of  $\frac{2.34}{2.34+4.46} \times 100 = 34.4\%$ . Although the depressurization provides the potential of degassing by controlling the solubility limit, it may take a long time for the super-saturated condition to arrive at the equilibrium condition.

### Gas Strip through Vapor-Bubbles

Gas stripping is a common way of removing specific solute from solvent. For example, pure nitrogen bubbles are often used to eliminate the oxygen content dissolved in liquids. The principle behind the gas stripping is diffusion. Now, instead of using gas like nitrogen, why not using vapor bubbles for extracting dissolved gases? For pure water, once evaporated, would have only water vapor and the concentration of other dissolved gases like oxygen and nitrogen may be considered to be virtually nil, which drives the diffusion of dissolved gases from the liquid water to the gaseous vapor. Further, once the condition for condensation for water is available, then this water vapor readily condenses to liquid water, while dissolved gases can be separated from the water body. Issues on the behavior of vapor bubbles are recently reviewed by Prosperetti.<sup>11</sup>

The driving mechanism of mass transfer in this case is diffusion that is governed by the Fick’s law, which states that the mass transfer rate is proportional to the contact area and the concentration gradient, with a proportionality constant called diffusion coefficient in Eq. (6).



**Figure 3.** Vapor Pressure of Water with respect to Temperature (Data from Ref. [12])

$$J = D \frac{dc}{dx} \tag{6}$$

Here  $J$  represents the diffusion flux ( $\frac{\text{mole}}{\text{m}^2\text{s}}$ ),  $D$  the diffusion coefficient, and  $\frac{dc}{dx}$  the concentration gradient, respectively. For multi-phase systems as bubble-diffusion, a modified version of the relation as shown in Eq. (7) is applicable, in which, instead of using the concentration gradient, difference in concentration between the phase, that is, between the inside vapor bubble and the outside liquid water body, are used with a due proportionality constants as shown in McGinnis et al <sup>13</sup>:

$$J = K_L(C_s - C) \tag{7}$$

where  $K_L$  = liquid-side mass transfer coefficient  
 $C_s$  = equilibrium concentration at vapor/water interface  
 $C$  = concentration of aqueous phase.

**Vapor-Bubble Generation**

Vapor bubbles are virtually cavitation bubbles that may appear when the local pressure diminishes down below the vapor pressure of the liquid. It is to be emphasized that the vapor pressure of water is a function of temperature and is illustrated in Figure 3. In a usual case, the cavitation bubbles are generated at the suction side of the impeller blades as in the case of the propeller of ships. In the present study, we do this in two steps. First, we lower the tank pressure down as low as 0.1 atm by using a vacuum generator, and then use a generic micro-bubble generator that provides the additional necessary pressure drop to reach out below the vapor pressure of water to generate cavitation bubbles. The advantage of lowering the environmental pressure in advance is in that the necessary pressure drop by the micro-bubble generator to generate the desired vapor bubbles can be minimized, which results in the required input energy as low as possible.

**The Effect of Bubble Size on the Diffusion Rate**

In dealing with the bubble diffusion,<sup>14</sup> it is necessary to consider the bubble size and its distribution along with the shape. Assuming uniform-sized spherical bubbles are generated through a bubbler, the relation among the bubble size in terms of its radius, surface area and the number of bubbles when a constant volume of air is

supplied, can be established as shown in Table 2, which indicates that the surface area is inversely proportional to its diameter. Assuming a constant air mass flow rate of  $Q$  supplied to generate bubbles of uniform radius  $r$ , the number of generated bubbles  $n_B$  and the resulting bubble surface area  $A_B$  are obtained as follows:

$$n_B = \frac{3Q}{4\pi r^2} \tag{8}$$

and

$$A_B = \frac{3Q}{r} \tag{9}$$

noting that  $Q = n_B \frac{4}{3} \pi r^3$  and  $A_B = n_B 4\pi r^2$ .

The residence time of the bubble in water depends on its diameter and the depth of origin. Under the assumption that the diameter of the spherical bubble remains almost constant during the rising, it could be expected that as the bubble origin becomes deeper and deeper, the residence time would increase accordingly, which eventually results in higher mass transfer. Figure 4 illustrates the bubble rise model and the free-body-diagram<sup>15</sup> of underwater bubbles.

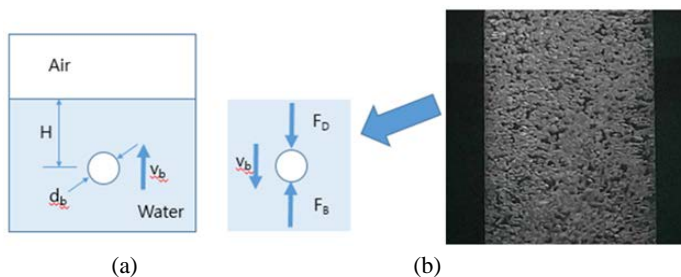


**Figure 4.** (a) Bubble rise model and (b) the free-body-diagram of underwater bubble.

**Table 2.** Relation between the radius and the surface area of spherical bubbles given a constant volume

Radius (mm)	No. of bubbles	Volume (mm <sup>3</sup> )	Surface area (mm <sup>2</sup> )	Surface area ratio
10	1/1,000	4.189	1.2566	1/10
1	1	4.189	12.566	1
0.1	1,000	4.189	125.66	10
0.01	1,000,000	4.189	1,256.6	100

**METHOD OF APPROACH**

**Test Apparatus and Testing Procedure**

Figure 5 illustrates the test apparatus used in the present study. It is composed of a sealed water tank with a depressurization system, a micro-bubble generator, a gas collector hood, and measurement system.<sup>16,17</sup> The water tank is 0.65m(L) x 0.65m(W) x 1.0m(H) in

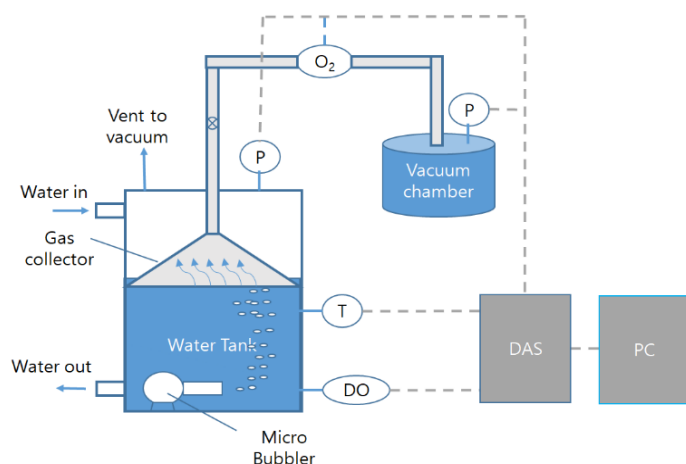


**Figure 5.** A Diagram of the Test Apparatus for Capturing and Measuring Extracted Gas from Water

size and is equipped with two large viewing windows as shown in Fig. 6. The tank, which is designed for low pressure operation with perfect seal so it can maintain vacuum state long enough as needed, is modified to capture the extracted dissolved gas by adopting a gas collector hood system for the present study.<sup>18</sup>

Depressurization is achieved by using a vacuum generator (E-Hwa Techno Ltd., FOCUS EV-15HS) which is connected to a 5-HP compressor for air supply. A micro-bubble generator with a counter-rotating blades fabricated using a 3D printer system (Stratasys Dimension sst 1200es) at the Future Automotive Intelligent Electronics Core Technology Center in Kongju National University is installed at the outlet of a DC driven small water pump (Daehwa Electric, Model DPW69-12, 12V DC, 69 l/min). This unit starts generating micro-bubbles under a certain tank pressure level. A gas collector hood collects the gas from uprising vapor bubbles during the depressurization process and the micro-bubble generation. It is made of transparent acrylic panel so that the water level both inside and outside of the hood becomes visible. A measurement scale is attached on one of the slanted side wall, as shown in Figure 7(a) and 7(b). Water level inside the hood defines the collected gas volume for which a calibration curve for the gas volume vs. the scale level is generated as shown in Figure 7(c). The calibration values are obtained by using the volume measuring function of a 3-dimensional CAD tool and verified through actual measurements. The maximum volume this hood may hold is set up for the present study that corresponds to 23cm of displacement on scale.

For the measurement of oxygen concentration of the collected gas, the collected gas need to flow through the oxygen sensor (Alpha-Omega O2 Monitor, 0~6 V, 0~100 %). A gas line from the hood to a vacuum tank with pressure and volume control devices are established for this purpose. D.O. sensor (Mettler-Toledo M-300 Transmitter, 0~6 V, 0~100 %) is inserted 0.1m above the bottom surface of the tank. Tank pressures and the temperatures of the water and the ullage are also measured by using a digital pressure transducer(ULFA Technology, SDT Series B760H) and K-type thermocouples, respectively. All the measured data are recorded using a data acquisition system(Yokogawa DA-100, 30



**Figure 6.** Test Apparatus showing the Water Tank with a Gas Collector inside

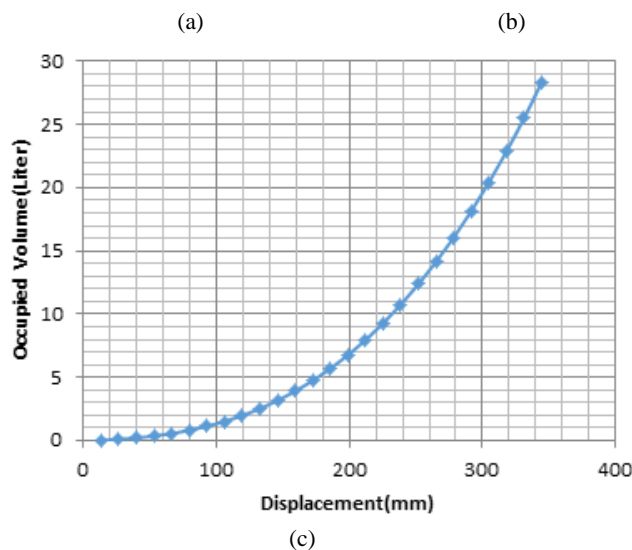
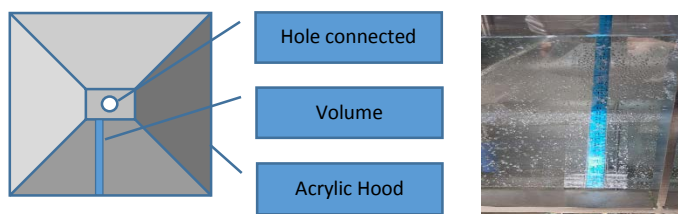


**Figure 7.** Gas Collector (a) Overall Configuration, (b) Measurement Scale at Work, (c) Relation between the Measured Displacement and the Volume.

ch.) and saved every 30 seconds. In addition, air bubblers are installed in order to initialize the test conditions.

The testing procedure for degassing and measurement is illustrated in Figure 8. Once the sensors<sup>19</sup> for oxygen and dissolved oxygen measurements are calibrated at room condition (0), fresh water is filled in the tank up to the desired level (1) and, if necessary, aeration using the air bubblers are conducted. Now, the initial dissolved oxygen concentration (IDOC) is measured (2).<sup>20</sup> Then the tank is depressurized down to 0.1 atm via the vacuum

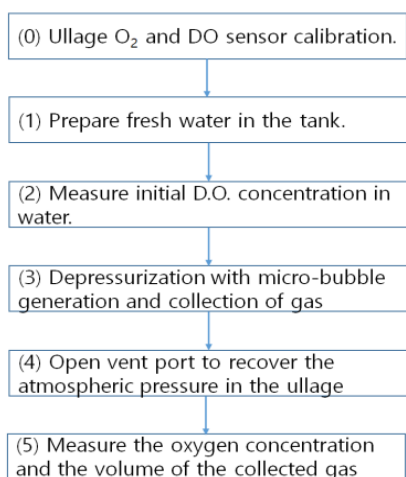


**Figure 8.** Testing Procedure for Degassing and Measurements

generator with the micro-bubbler being operated and the bubbles are then captured under the gas collector hood (3). Once the displacement marked by the inner hood water level scale reaches the maximum value of 23 cm, the micro-bubbler operation is stopped, and the vent is opened to recover the pressure level back to the atmospheric level (4). For the volume occupied by the gas changes with temperature and pressure, it is necessary that the measurement conditions are fixed. In the present study, the volume measurement is done at a room condition. The captured air volume (CAV) of the collected gas is measured by reading the displacement marked by the inside-the-hood water level while the captured air oxygen concentration (CAOC) of the collected gas is measured by letting the collected gas flow through the oxygen sensor (Alpha-Omega O<sub>2</sub> Monitor) (5). Although there exists some difference between the water levels inside and outside, the contribution of the water level difference is regarded to be relatively small (less than 18 cm in water level scale) and negligible in the present study. Finally, the dissolved oxygen concentration (FDOC) is measured.

#### Test Conditions and Methods

According to the testing procedure described in the previous section, the oxygen sensor and the D.O. sensor are calibrated to read 20.9 % at room temperature of 17 °C (0). Fresh tap water of 296 liters occupies 70 % of the total volume of the water tank (1). The water D.O. concentration was initially read to be 17.2 %. After 30 minutes of aeration at 30 slpm, the D.O. reading reached 19.5 % then stabilized at 18.6 % after stopping the air supply. In order to measure the gas volume and the concentration through the present degassing process, the air gas initially present on the hood is eliminated by letting this gas vent out through the vent hole on the top of the vent hood. The gas volume in the gas line from the vent hole to the first valve is estimated to be 9.2 cm<sup>3</sup> (total line length of 73 cm with 4 mm I.D.). The information on this in-line gas is used for properly estimating the captured volume and the oxygen concentration of the captured gas. In order to demonstrate the difference between the depressurization only and the combined depressurization along with bubble diffusion, the tests are conducted in two steps, i.e., (1) case I: depressurization only (0.1 atm or 10 kPa) and case II: depressurization combined with bubble generation.

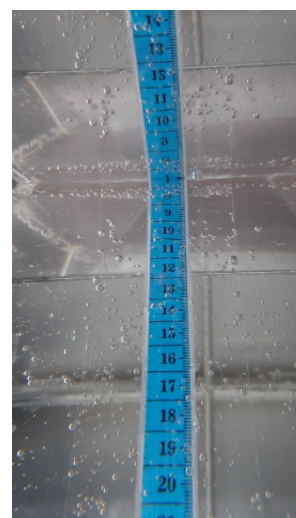


**Figure 9.** Captured Gas and the Water-Level-Scale for Volume Measurement (11.8mm @57 min. after Depressurization)

## RESULTS AND DISCUSSION

### Case I Results: Depressurization down to 0.1 atm (10kPa)

Table 3 shows the test results of depressurization-only-case. Starting with D.O. level of 18.6 % at atmospheric pressure (measured pressure of 100 kPa), the tank pressure is reduced to 10 kPa in 25 minutes and the water level is measured to be 10.5 cm. Degassing through the vacuum generator is continued for additional 32 minutes resulting in the increase of the gas volume inside the hood as seen in Figure 9. As the depressurization progresses, bubbles originate from the bottom and the wall surfaces and grow in size, then are detached from the wall surface to move upward to the collecting hood, but the volume increase was observed very slow. After monitoring the initial 57 minutes of depressurization, the tank pressure is recovered to the atmospheric pressure for volume measurement of the extracted dissolved gas, which results in the shrink of the gas volume as shown in Table 3. The total volume of degassed air out of 296 L of water is found to be 0.20 L excluding the line volume under 1 atm condition at room temperature, which results in 0.00067 L-air/L-water or 0.067% of the water volume.

### Case II Results: Vapor Bubble Generation and Depressurization down to 0.1 atm (10kPa)

After the depressurization only tests, a combined degassing process with vapor bubble generation is further conducted.<sup>21</sup> Considering the capacity of the capture hood (max. 23cm in water level scale), the degassing process is repeated five times to estimate the total available gas from the test water of 296 liter as shown in Table IV. The time required to fill up the hood varied from less than an hour in the early rounds to over two hours in the later rounds. After each round of low pressure degassing, the tank pressure is recovered to atmospheric pressure before the water surface level is recorded, from which the gas volume inside the hood is calculated. According to the test results, it was possible to capture the total volume of 5.894 liter at 100kPa (0.020 L-air/L-water or 2.0% of the water volume) and the volume averaged oxygen concentration was 29.9%. Figure 10 shows the measured oxygen concentration which

**Table 3.** Degassed Air Measurement Results with Depressurization at 0.1 atm (10 kPa)

Test Date	Test Condition Description			
11/27/20	Before depressurization	After 25 min. of depressurization	After 57 min. of depressurization	Pressure recovered to 1 atm
Tank pressure (outside the hood)	100kPa	10kPa	10kPa	100kPa
Water surface level(cm)	0	10.5	11.8	3.7
Gas volume(liter)	0.009*	1.492+0.009*	1.940+0.009*	0.199+0.009*
Oxygen concentration(n%)	20.9	Not measured	Not measured	Not measured
D.O. concentration(n%)	18.6	N.A.	N.A.	Not measured

\* the line volume of 9 cm<sup>3</sup>

demonstrates the change of the oxygen concentration of the captured degassed air. As the bleeding begins through the oxygen sensor, the oxygen concentration at calibrated value of 20.9% increase to steady values as shown in Figure 10 and Table 4.

**Mass Balance of Degassed Oxygen and D.O. Concentration**

If the dissolved gas in water is under an equilibrium condition with the idealized air with 79.1% of nitrogen and 20.9% of oxygen, the amount of dissolved nitrogen and oxygen can be estimated using equations (1) through (5). For the water volume of 0.65m x 0.65m x 0.7m = 0.296m<sup>3</sup> = 296 liter in the tank, the expected amount of dissolved nitrogen and oxygen from the equations (4) and (5) are

$$m_{O_2} = G_{O_2} V_w = 8.32 \frac{mg}{L} \times 296L = 2,462mg = 2.462g$$

and

$$m_{N_2} = G_{N_2} V_w = 13.89 \frac{mg}{L} \times 296L = 4,111mg = 4.111g.$$

The volume that may be occupied by these gases under an atmospheric pressure become

$$V_{O_2} = \frac{m_{O_2} R_{O_2} T}{P} = \frac{2.462 \times 10^{-3} kg \times 0.2598 kJ/kgK \times 298K}{101.3 kPa} = 0.00188m^3$$

and

$$V_{N_2} = \frac{m_{N_2} R_{N_2} T}{P} = \frac{4.111 \times 10^{-3} kg \times 0.2968 kJ/kgK \times 298K}{101.3 kPa} = 0.00359m^3,$$

which results in the total of 5.47 liter. For the total volume of extracted gas from the experiments is 5.894 liter, it seems that the extracted gas volume exceeds the expected dissolved gas amount

**Table 4.** Degassed Air Measurement Results with Vapor Bubble Diffusion with Depressurization at 0.1 atm (10kPa)

Test Date	Test Condition Description				
11/27/20, 11/28/20, 12/4/20, 12/5/20	Round 1	Round 2	Round 3	Round 4	Round 5
Tank pressure (outside the hood)	100kPa	100kPa	100kPa	100kPa	100kPa
Water surface level(cm)	9.4	9.2	10.2	9.2	9.1
Gas volume (liter)	1.172+0.009*	1.114+0.009*	1.405+0.009*	1.114+0.009*	1.089+0.009*
Oxygen concentration(%)	31.0	31.9	30.5	29.3	27.7
D.O. concentration(%)	15.2	10.8	9.5	7.3	5.5

\* the line volume of 9cm<sup>3</sup>

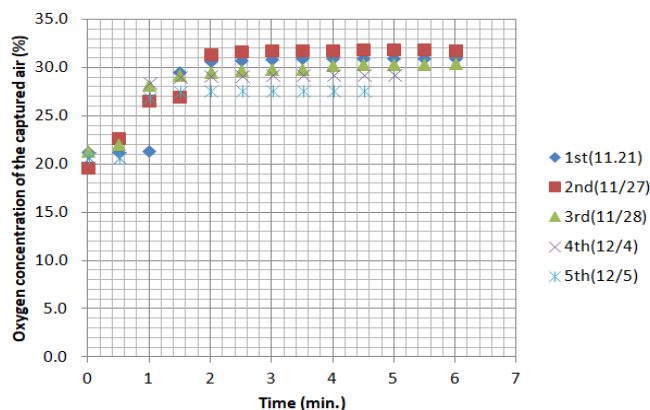


**Figure 10.** Measured Oxygen Concentration of Extracted Degassed Air

based on the solubility data at 25°C. However, noting that actual temperature of water during the experiments was about 17°C, the solubility was re-evaluated. Figure 11 demonstrates the temperature dependency of solubility of oxygen and nitrogen in water based on the correlation by McGinnis et al.<sup>13</sup> According to this solubility correlation (Table V), the solubility of oxygen and nitrogen at 17°C water are greater than those at 25°C by 16.9% and 14.2%, respectively, which tells that the total volume of dissolved gas be 6.298 liters (2.198 liter of oxygen and 4.100 liter of nitrogen, respectively). Considering this volume as the total available dissolved gas, the captured gas amount in the present study would be 93.6% of the total available dissolved gas.

Regarding the mass balance, the total assumed initial mass of oxygen dissolved in 296 L saturated water body at 17°C is 0.08897 mole (1.993 L) resulting in 9.62 mg/L while the measured extracted oxygen through the present experiments is 0.07867 mole (1.762 L = 5.894 L x 0.299), leaving 0.0103 mole (0.231 L) still dissolved in water, which is equivalent to DO concentration of 1.11 mg/L. However, the measured DO concentration reading after the experiment is found to be 5.5 mg/L, which is higher than expected. In this regard, the issue of mass balance needs to be studied further with a more reliable measurement system. In the present experiments, the DO measurement during the depressurization and bubbling process is avoided because of the undesired intervention of bubbles in DO measurement, and is conducted upon completion of every depressurization and tank pressure recovery to the atmospheric pressure, after refreshing the sensor out of the water body.

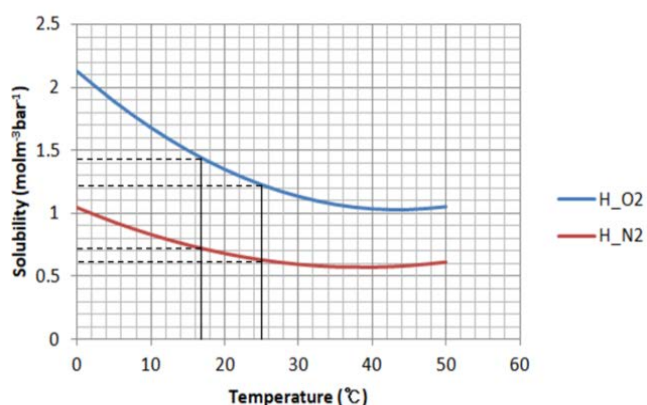


**Figure 11.** Solubility of Oxygen and Nitrogen in Water at Different Temperature [13]

**Table 5.** Henry's Constants for Various Gases in Water at 25°C. Ref [13]

Correlation equation (T in °C)
$H_{O_2} (\text{mol} \cdot \text{m}^{-3} \cdot \text{bar}^{-1})$ $= 2.125 - 5.021 \times 10^{-2}T + 5.77 \times 10^{-4}T^2$
$H_{N_2} (\text{mol} \cdot \text{m}^{-3} \cdot \text{bar}^{-1})$ $= 1.042 - 2.450 \times 10^{-2}T + 3.171 \times 10^{-4}T^2$

## CONCLUSIONS

In the present study, a gas stripping based on vapor bubble diffusion is proposed and the extraction of dissolved gas from water with volume and concentration measurement is experimentally conducted. In order to generate micro-bubbles, a process combined with depressurization and a genuine micro-bubble-generation is applied. Through the present study, the possible limit of extractable amount of dissolved gas in water and the oxygen concentration of the extracted gas mixture is successfully identified through the experiment.

According to the present experimental results, a total of 5.9 liter of gas is extracted out of 296 liter of water at the test room temperature of 17°C. The volume averaged oxygen concentration of the extracted gas is found to be 29.9%, which is close to the the

expected higher oxygen concentration of 34% out of the saturated water at reference 25°C. The process featured by the combination of depressurization and micro-bubble generation is unique not only in that it does not require any third chemicals in degassing, but also in that the degassing potential is high enough because the diffusion with a concentration difference against a virtual zero concentration of the vapor bubbles is conceivable.

The higher oxygen content gas or oxygen-enriched-air from water, once obtainable without too much cost, may find diversified applications from artificial gills, underwater shelter, and submarines to auxiliary oxygen supply for various types of human dwelling. Further study may include but not limited to the uncertainty analysis for this process along with DO measurement at lower concentration and bubbly environment, cost analysis, sensitivity analysis and parameter studies for device optimization or selection for micro-bubble-generators.

## ACKNOWLEDGMENTS

Authors appreciate the contribution of Mr. Jin-Goo Kim whose life-long experience and insight paved a safe and concrete way of achieving the finest experimental data. This work was supported by the research grant of Kongju National University in 2021.

## REFERENCES

1. J. Lee, P.W. Heo, T. Kim. Theoretical model and experimental validation for underwater oxygen extraction for realizing artificial gills. *Sensors Actuators, A Phys.* **2018**, 284, 103–111.
2. G.R. Greenbank, P.A. Wright. The Deaeration of Raw Whole Milk before Heat Treatment as a Factor in Retarding the Development of the Tallowy Flavor in its Dried Product. *J. Dairy Sci.* **1951**, 34 (8), 815–818.
3. Aeration and gas stripping <https://ocw.tudelft.nl/wp-content/uploads/Aeration-and-gas-stripping-1.pdf>. (Accessed on June 3, 2021).
4. A. Daniel. How does deaerator work? <https://watertreatmentbasics.com/how-does-deaerator-work/>.
5. M.C. Yang, E.L. Cussler. Artificial gills. *J. Memb. Sci.* **1989**, 42 (3), 273–284.
6. P. Magee. Circle (CO2 reabsorbing) breathing systems: Human applications. *Proc. Inst. Mech. Eng. Part H J. Eng. Med.* **2017**, 231 (7), 617–624.
7. R. Kumar, M.P. Chaudhary, M.A. Shah, K. Mahajan. A mathematical elucidation of separation membrane operations and technology of chemical and physical processes: An advanced review. *J. Integr. Sci. Technol.* **2020**, 8 (2), 57–69.
8. P. Costa, A. Ferro, E. Ghiazza, B. Bosio. Seawater deaeration at very low steam flow rates in the stripping section. *Desalination* **2006**, 201 (1–3), 306–314.
9. G. Ming, D. Zhenhao. Prediction of oxygen solubility in pure water and brines up to high temperatures and pressures. *Geochim. Cosmochim. Acta* **2010**, 74 (19), 5631–5640.
10. A. Braibanti, E. Fiscaro, C. Compari. Solubility of oxygen and inert substances in water. *Polyhedron* **2000**, 19 (24–25), 2457–2461.
11. A. Prosperetti. Vapor Bubbles. *Annu. Rev. Fluid Mech.* **2017**, 49, 221–248.
12. D.R. Lide. CRC Handbook of Chemistry and Physics; CRC Press, **2004**.
13. D.F. McGinnis, J.C. Little. Predicting diffused-bubble oxygen transfer rate using the discrete-bubble model. *Water Res.* **2002**, 36 (18), 4627–4635.
14. Q. Wang, Y. Liu, J. Luo, et al. Experimental research on the performance of a gas lift bubble pump based on a diffusion generation process. *Appl. Therm. Eng.* **2021**, 182, 116060.
15. R.F.L. Cerqueira, E.E. Paladino, F. Evrard, F. Denner, B. van Wachem. Multiscale modeling and validation of the flow around Taylor bubbles surrounded with small dispersed bubbles using a coupled VOF-DBM approach. *Int. J. Multiph. Flow* **2021**, 141, 103673.

16. Y. Du Jun, J.S. Lee. A new safe approach of evaluating the oxygen transfer efficiency (OTE) of underwater bubble diffusion. *J. Green Eng.* **2020**, 10 (7), 4154–4165.
17. J.-A. Hong, J.-S. Lee, Y.-D. Jun. Characterization of Extracted Dissolved Gas from Water. *J. Human-centric Sci. Technol. Innov.* **2021**, 1 (2), 23–30.
18. S.B. Kondawar, A.M. More, H.J. Sharma, S.P. Dongre. Ag-SnO<sub>2</sub>/Polyaniline composite nanofibers for low operating temperature hydrogen gas sensor. *J. Mater. Nanosci.* **2017**, 4 (1), 13–18.
19. B.S. Chhikara, R.S. Varma. Nanochemistry and Nanocatalysis Science: Research advances and future perspectives. *J. Mater. Nanosci.* **2019**, 6 (1), 1–6.
20. O. Kisi, M. Alizamir, A.D. Gorgij. Dissolved oxygen prediction using a new ensemble method. *Environ. Sci. Pollut. Res.* **2020**, 1–15.
21. M. Kostoglou, T.D. Karapantsios. Bubble dynamics during the non-isothermal degassing of liquids. Exploiting microgravity conditions. *Adv. Colloid Interface Sci.* **2007**, 134–135, 125–137.